

# SUPPLEMENTARY INFORMATION

## **Polymeric carbon nitride coupled with a molecular thiomolybdate catalyst: exciton and charge dynamics in light-driven hydrogen evolution**

Ashwene Rajagopal,<sup>a</sup> Elham Akbarzadeh,<sup>a,j</sup> Chunyu Li,<sup>b,c</sup> Dariusz Mitoraj,<sup>d</sup> Igor Krivtsov,<sup>d,\*</sup>

Christiane Adler,<sup>d</sup> Thomas Diemant,<sup>e</sup> Johannes Biskupek,<sup>f</sup> Ute Kaiser,<sup>f</sup> Changbin Im,<sup>d</sup> Magdalena

Heiland,<sup>a</sup> Timo Jacob,<sup>d,g,h</sup> Carsten Streb,<sup>a,g,h\*</sup> Benjamin Dietzek,<sup>b,c,i</sup> \* Radim Beranek<sup>d,\*</sup>

<sup>a</sup> Institute of Inorganic Chemistry I, Ulm University, Albert-Einstein-Allee 11, 89081 Ulm, Germany

<sup>b</sup> Institute of Physical Chemistry and Abbe Center of Photonics, Friedrich Schiller University Jena, Lessingstr. 10, 07743 Jena, Germany

<sup>c</sup> Department Functional Interfaces, Leibniz Institute of Photonic Technology (IPHT), Albert-Einstein-Str. 9, 07745 Jena, Germany

<sup>d</sup> Institute of Electrochemistry, Ulm University, Albert-Einstein-Allee 47, 89081 Ulm, Germany

<sup>e</sup> Institute of Surface Chemistry and Catalysis, Ulm University, Albert-Einstein-Allee 47, 89081 Ulm, Germany

<sup>f</sup> Electron Microscopy of Materials Science, Central Facility for Electron Microscopy, Ulm University, Albert-Einstein-Allee 11, 89081, Ulm, Germany

<sup>g</sup> Helmholtz-Institute-Ulm (HIU), Helmholtzstr. 11, 89081, Ulm, Germany

<sup>h</sup> Karlsruhe Institute of Technology (KIT), P.O. Box 3640, 76021, Karlsruhe, German

<sup>i</sup> Center for Energy and Environmental Chemistry Jena (CEEC Jena), Philosophenweg 7a, 07743 Jena, Germany

<sup>j</sup> Department of Chemistry, Sharif University of Technology, Tehran, Iran

\*Corresponding authors: [igor.krivtsov@uni-ulm.de](mailto:igor.krivtsov@uni-ulm.de), [carsten.streb@uni-ulm.de](mailto:carsten.streb@uni-ulm.de),  
[benjamin.dietzek@uni-jena.de](mailto:benjamin.dietzek@uni-jena.de), [radim.beranek@uni-ulm.de](mailto:radim.beranek@uni-ulm.de)

### Preliminary photocatalytic study:

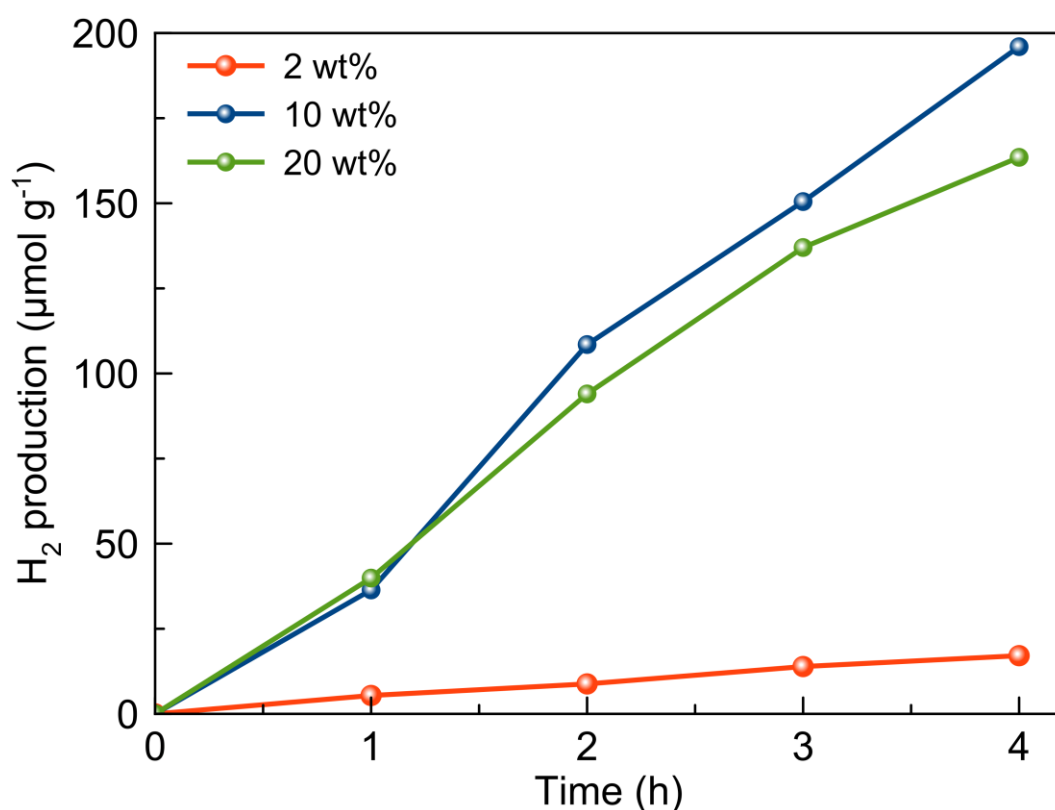


**Figure S1.** Photocatalytic HER performed using CN<sub>x</sub> based materials with varied loading of {Mo<sub>3</sub>} clusters under 420 nm irradiation. Conditions: [catalyst]: 10 mg, Solvent: 10 ml H<sub>2</sub>O:MeOH (9:1, v:v). Note that the hydrogen production rates in these preliminary measurements were lower than in the rest of the study due to a difference in geometry of the reaction cell which resulted in different absorbed photon flux.

### FTIR analysis:

FT-IR spectra of CN<sub>x</sub>, Na<sub>2</sub>[Mo<sub>3</sub>S<sub>13</sub>] and {Mo<sub>3</sub>}@CN<sub>x</sub> nanocomposite are displayed in Figure 1b. In the FT-IR spectrum of CN<sub>x</sub> and {Mo<sub>3</sub>}@CN<sub>x</sub> hybrid the peaks at around 1639 cm<sup>-1</sup> can be ascribed to C–N stretching vibration modes and the peaks at 1245, 1329 and 1416 cm<sup>-1</sup> are attributed to the aromatic C–N stretching. The sharp peak at 806 cm<sup>-1</sup> is related to the out-of-plane bending vibration of heterocyclic C–N. The broad peak at around 2900–3400 cm<sup>-1</sup> can be related to the stretching modes of the N–H bond and the hydroxyl group of the adsorbed water. For the pure Na<sub>2</sub>[Mo<sub>3</sub>S<sub>13</sub>], the spectrum displays a sharp peak at 1138 cm<sup>-1</sup> which can be assigned to the SO<sub>4</sub><sup>2-</sup> group in the compound which probably is produced during the cation exchange process. However, no distinct sign of [Mo<sub>3</sub>S<sub>13</sub>]<sup>2-</sup> cluster is obvious in the FT-IR spectrum of {Mo<sub>3</sub>}@CN<sub>x</sub> composite, which can be because of the little amount of {Mo<sub>3</sub>} in the hybrid and also existence of CN<sub>x</sub>.

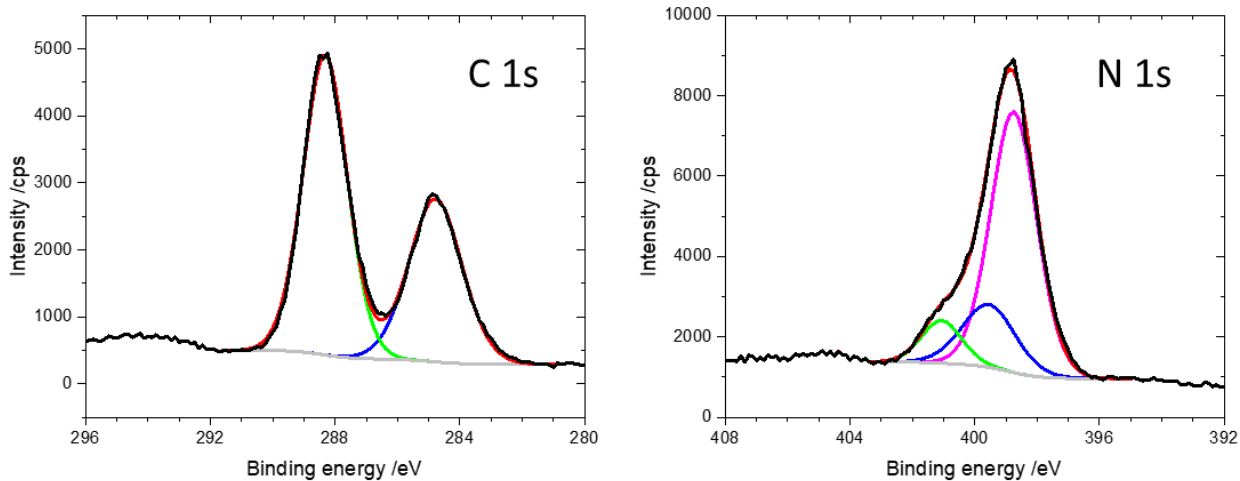


**Figure S2.** XPS C 1s and N 1s spectra of  $\text{CN}_x\text{-}\{\text{Mo}_3\}$

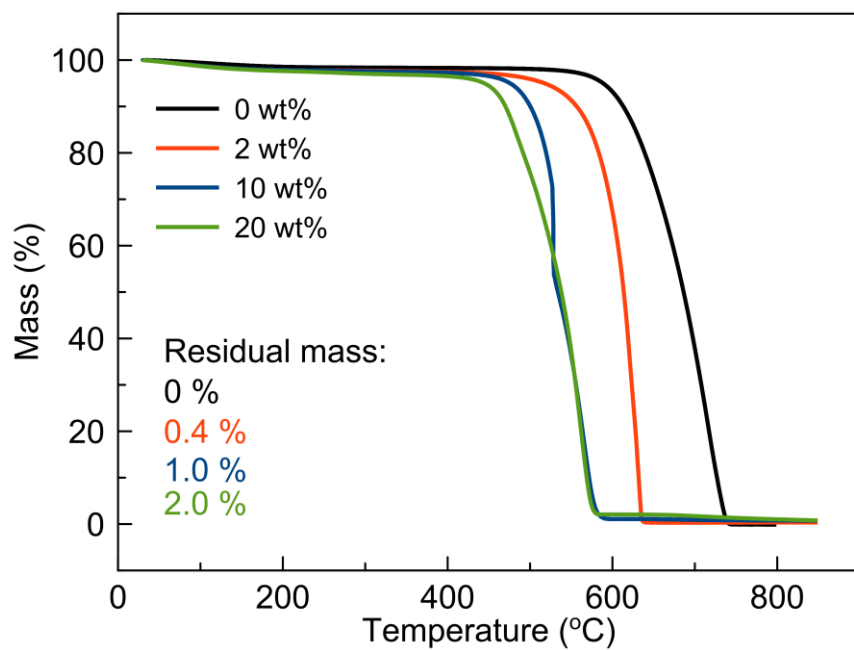


**Figure S3.** Thermogravimetric analysis of the  $\text{CN}_x$  materials with different  $\{\text{Mo}_3\}$  cluster loadings in air.

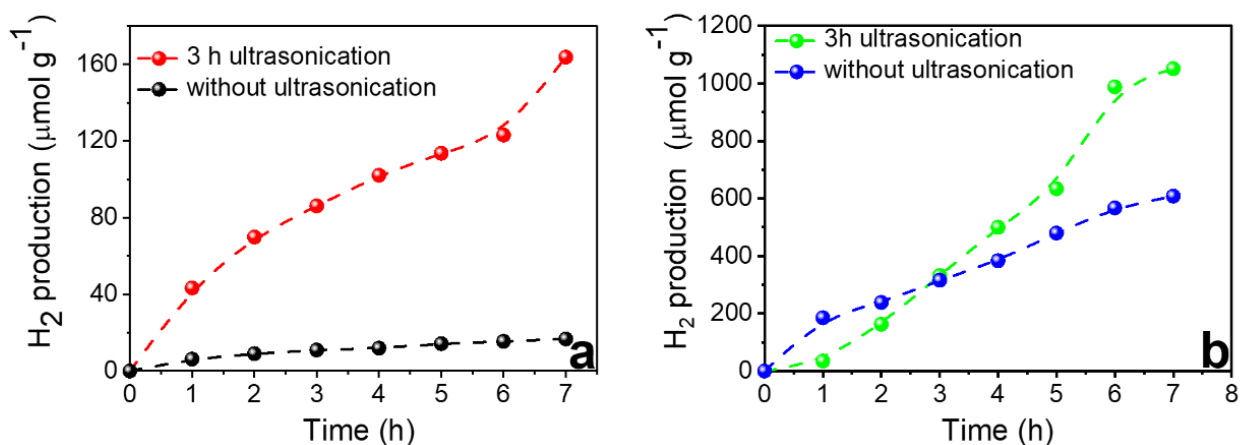


**Figure S4.** Effect of sonication on photocatalytic HER for (a) CN<sub>x</sub> and (b) CN<sub>x</sub>-{Mo<sub>3</sub>} under 420 nm irradiation. Conditions: [catalyst] : 10 mg, Solvent: 10 ml H<sub>2</sub>O:MeOH (9:1, v:v), in absence of any additional electron donors.

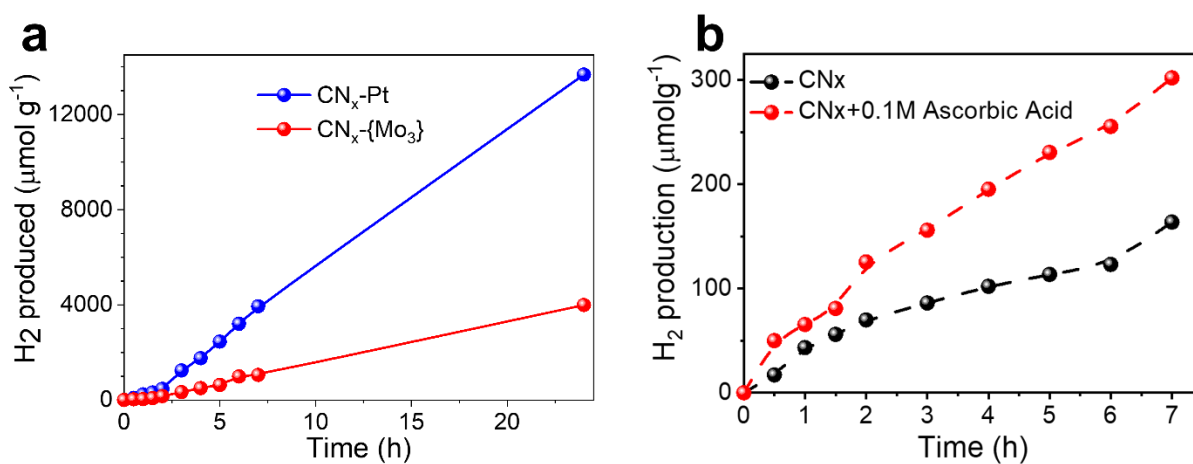


**Figure S5.** (a) H<sub>2</sub> evolution during long-term (24 hours) irradiation. (b) Effect of electron donor addition (0.1M ascorbic acid) on photocatalytic HER in presence of CN<sub>x</sub> under 420 nm irradiation. Conditions: [catalyst] : 10 mg, Solvent: 10 ml H<sub>2</sub>O:MeOH (9:1, v:v).

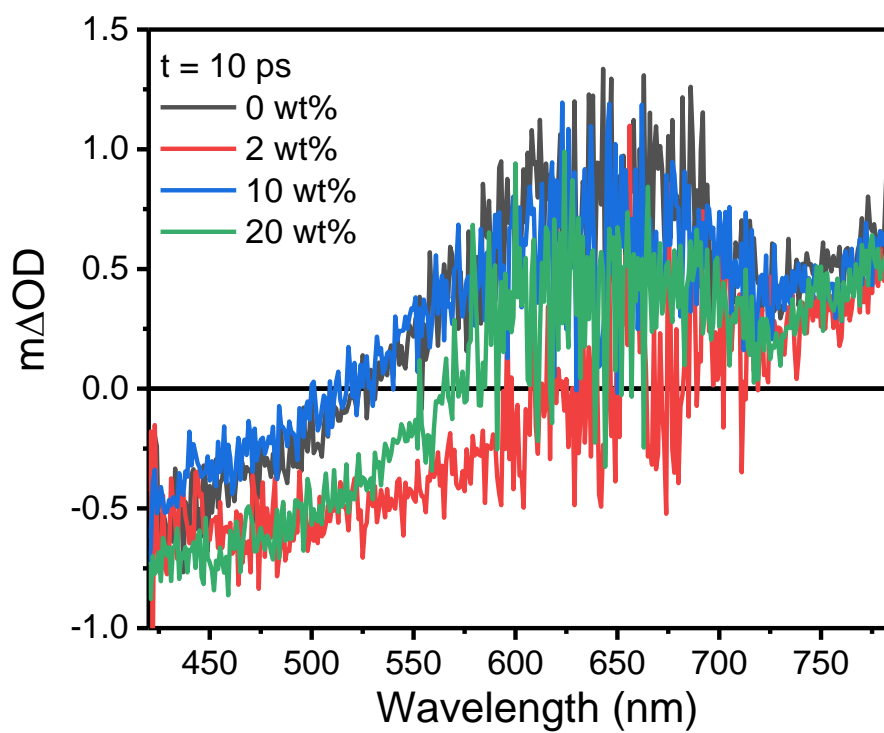


**Figure S6.** fs-TAS spectra of  $\text{CN}_x\text{-}\{\text{Mo}_3\}$  dispersions in  $\text{H}_2\text{O}$  upon excitation at 325 nm at 10 ps delay times. The figure displays the raw data.

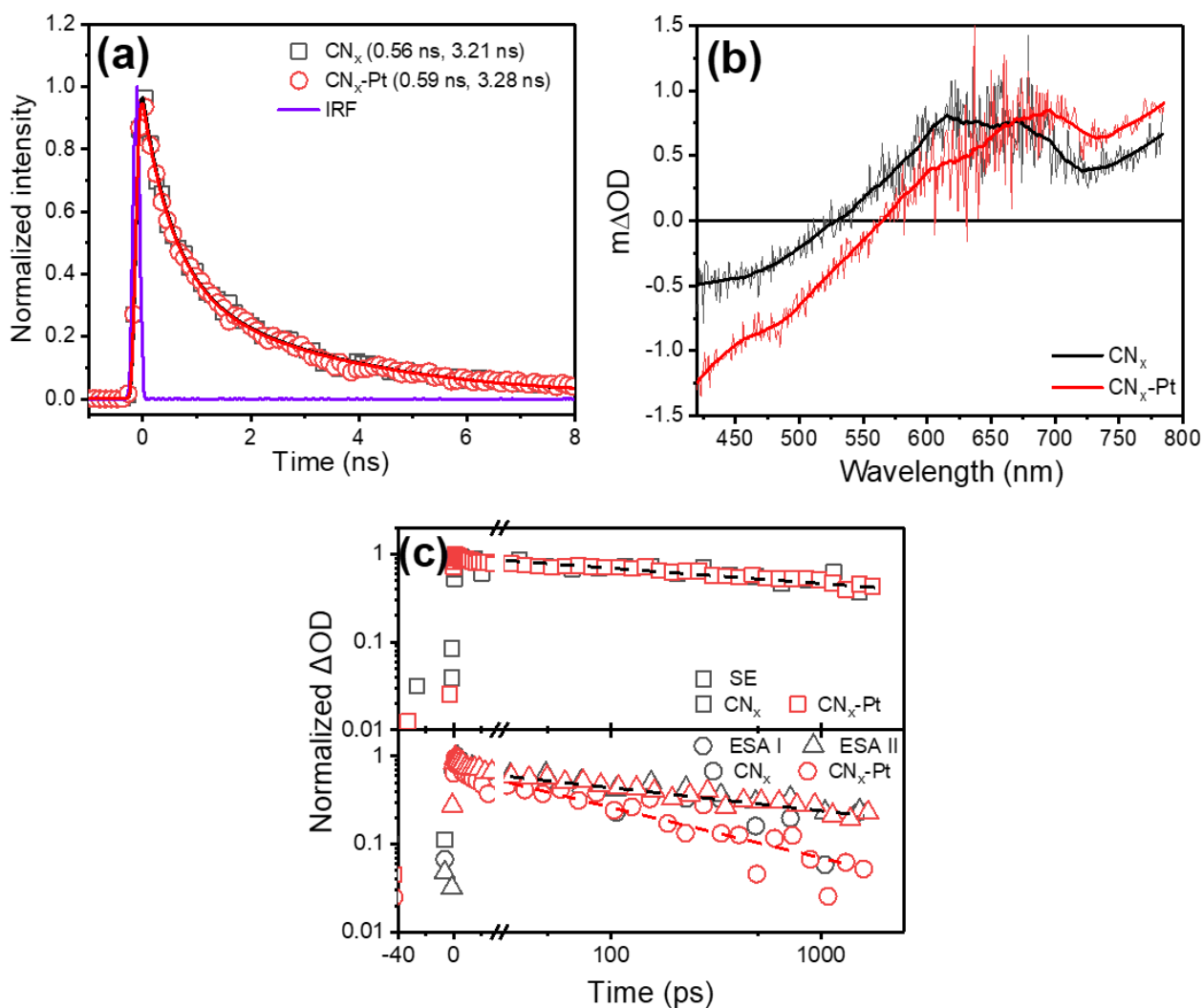


**Figure S7.** (a) Time-resolved photoluminescence decay curves of Pt functionalized  $\text{CN}_x$  samples after 385 nm photoexcitation. The samples were prepared by drop casting. (b) fs-TAS spectra at 10 ps delay of  $\text{CN}_x$ -Pt dispersions in  $\text{H}_2\text{O}$  upon excitation at 325 nm and corresponding (c) fs-TAS decay kinetics obtained by spectrally integrating the transient absorption data in different probe wavelength ranges. A quantitative analysis of the transient absorption data indicates, that the kinetics can be described by a power law model. The exponent of the power law is smaller than unity ( $\sim 0.43$ ), suggesting that trapping/detrapping plays a significant role in excited state dynamics of the  $\text{CN}_x$ -Pt samples. This is consistent with the comparably slow time scale for the recombination process.

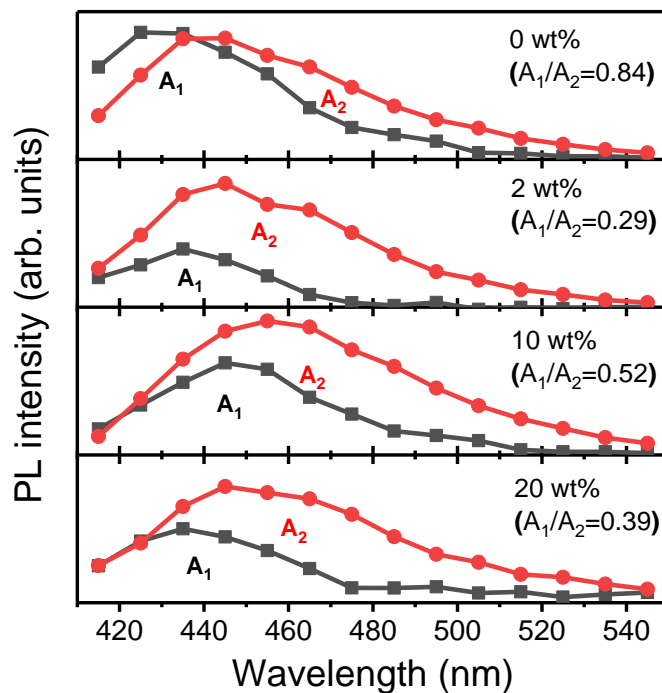


**Figure S8.** Species-associated emission spectra of  $\text{CN}_x\text{-}\{\text{Mo}_3\}$  with respective lifetimes (black lines present emission from the short-lived photoluminescence ( $\tau < 1\text{ ns}$ ), while the red spectra reflect the spectra distribution of the long-lived emission with lifetimes ranging from 3.0 to 5.5 ns). The lifetimes are obtained by a global fit of the two-dimensional streak camera data with a biexponential model. The experimental response function of the streak camera measurements is 0.06 ns wide.

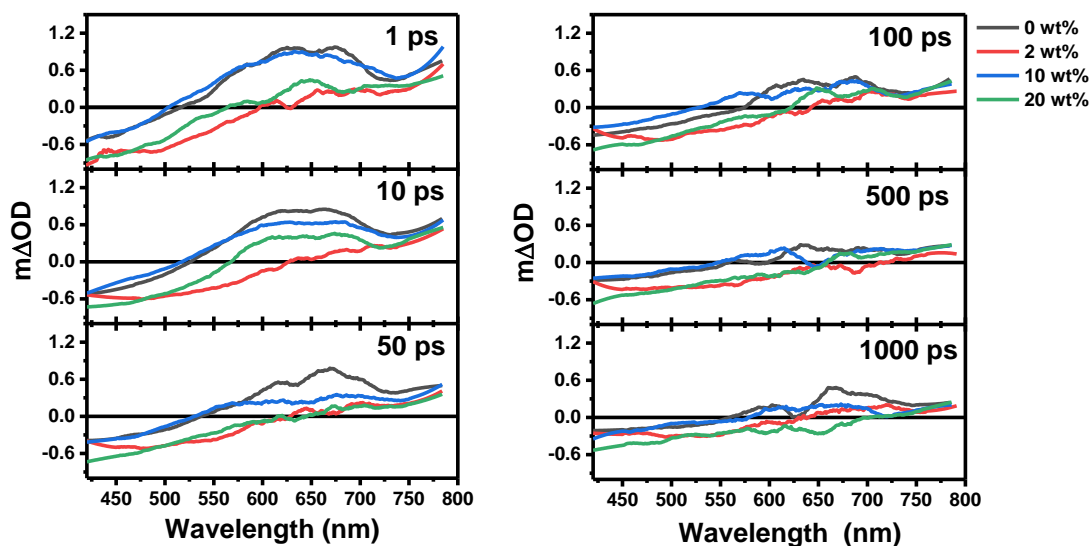


**Figure S9.** fs-TAS smoothed spectra of  $\text{CN}_x\text{-}\{\text{Mo}_3\}$  dispersions in  $\text{H}_2\text{O}$ . The spectra were recorded upon 325 nm excitation at different delay times.

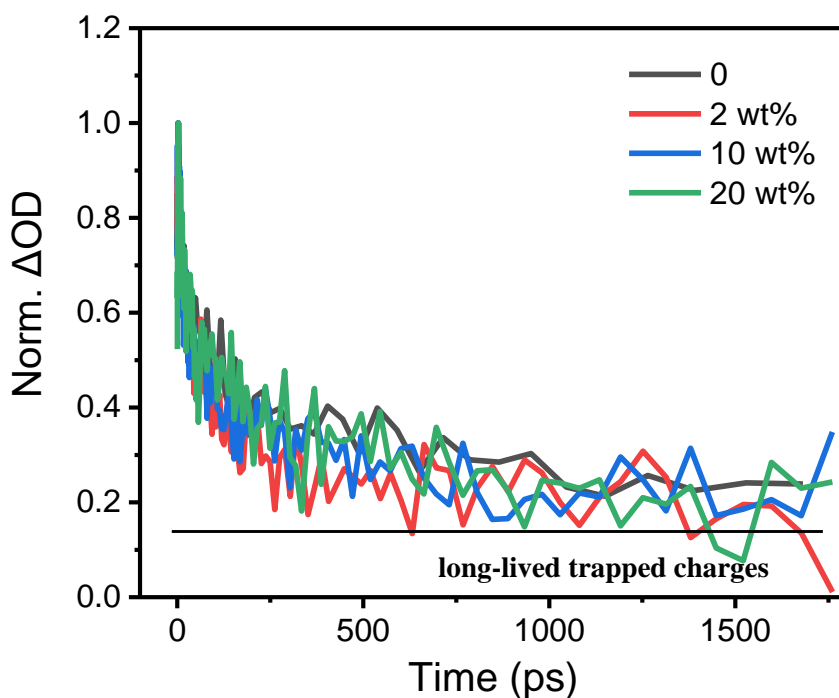


**Figure S10.** fs-TAS decay of  $\text{CN}_x\text{-}\{\text{Mo}_3\}$  dispersions in  $\text{H}_2\text{O}$  integrated within NIR regions upon 325 nm excitation.

### **Theoretical calculations:**

Density Functional Theory (DFT) calculations were performed using the Vienna Ab initio Simulation Package (VASP) version 5.4.4 using the projector-augmented wave (PAW) method to represent the basis set.<sup>1-5</sup> For accuracy of the electronic properties, the Heyd-Scuseria-Ernzerhof (HSE06) hybrid functional was employed.<sup>6,7</sup> The screening parameter  $m$  in HSE was set at  $0.2 \text{ \AA}^{-1}$  and the exchange parameter  $a$  was 0.25. Grimme's D3 dispersion correction was used to describe long range dispersive interactions.<sup>8,9</sup> The wavefunction was optimized to an accuracy of  $10^{-6} \text{ eV}$  while geometries were relaxed until the forces reached below  $5 \cdot 10^{-2} \text{ eV \AA}^{-1}$ . Gaussian finite-temperature smearing was employed with a smearing width of 0.01 eV. A plane wave energy cut-off of 400 eV for both  $\{\text{Mo}_3\}$  and  $\text{CN}_x$ . To offset the spurious interactions between the periodic images, vacuum was introduced along the  $z$ -direction ( $\sim 20 \text{ \AA}$ ) for  $\text{CN}_x$  and  $\{\text{Mo}_3\}$  was placed to the center of cubic vacuum box (40  $\text{\AA}$ ) with dipole corrections. Integration in the reciprocal space was performed on a  $5 \times 5 \times 1$  Monkhorst-Pack  $k$ -grid mesh. For implicit solvation effects in water, the GLSSA13 solvent model implemented in the VASPsol extension was invoked,<sup>10-12</sup> using a dielectric constant of bulk water at room temperature of 78.4.



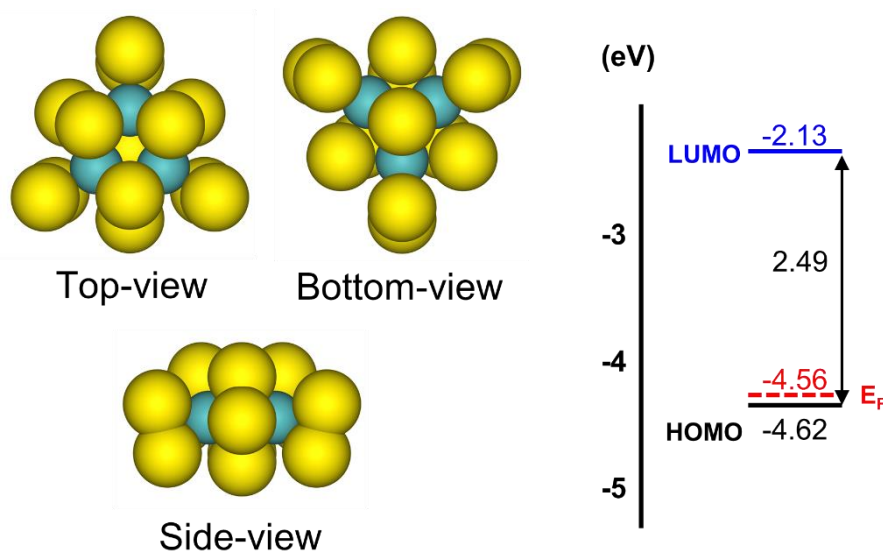


**Figure S11.** Scheme of the structure {Mo<sub>3</sub>} employed in DFT calculation and HOMO-LUMO energy.

## References

1. G. Kresse, J. Hafner, Phys. Rev. B 1993, 47, 558–561.
2. G. Kresse, J. Hafner, Phys. Rev. B 1994, 49, 14251–14269.
3. G. Kresse, J. Furthmüller, Comput. Mater. Sci. 1996, 6, 15–50.
4. G. Kresse, J. Furthmüller, Phys. Rev. B 1996, 54, 11169–11186.
5. G. Kresse, D. Joubert, Phys. Rev. B 1999, 59, 1758–1775.
6. Heyd, J.; Scuseria, G. E.; Ernzerhof, M. J. Chem. Phys. 2003, 118, 8207–8215.
7. Heyd, J.; Scuseria, G. E.; Ernzerhof, M. Erratum: Hybrid Functionals Based on a Screened Coulomb Potential [J. Chem. Phys. 118, 8207 (2003)]. J. Chem. Phys. 2006, 124, 219906.
8. S. Grimme, J. Antony, S. Ehrlich, and S. Krieg, J. Chem. Phys. 2010, 132, 154104.
9. Grimme, S. Ehrlich, and L. Goerigk, J. Comp. Chem. 2011, 32, 1456.
10. D. Gunceler, K. Letchworth-Weaver, R. Sundararaman, K. A. Schwarz, T. A. Arias, Model. Simul. Mater. Sci. Eng. 2013, 21, 074005.
11. K. Mathew, R. G. Hennig, ArXiv160103346 Cond-Mat 2016.
12. K. Mathew, R. Sundararaman, K. Letchworth-Weaver, T. A. Arias, R. G. Hennig, J. Chem. Phys. 2014, 140, 084106.